Available online at www.sciencedirect.com
ScienceDirect
Bioelectrochemistry 71 (2007) 172–179
Bioelectrochemistry
www.elsevier.com/locate/bioelechem

Direct electrochemistry and electrocatalytic characteristic of heme proteins immobilized in a new sol–gel polymer film

Yi-Xin Sun [a,b], Sheng-Fu Wang [a,*]

[a] *Ministry-of-Education, Key Laboratory for the Synthesis and Application of Organic Functional Molecules, and College of Chemistry and Chemical Engineering, Hubei University, Wuhan 430062, PR China*
[b] *School of Sciences, Zhejiang Forestry University, Lin'an 311300 PR China*

Received 5 October 2006; received in revised form 17 March 2007; accepted 7 April 2007
Available online 21 April 2007

Abstract

Heme proteins were immobilized on glass carbon electrodes by poly (*N*-isopropylac-yamide-co-3-methacryloxy-propyl-trimethoxysilane) (PNM) and exhibited a pair of well-defined, quasi-reversible cyclic voltammetric peaks at about −0.35 V versus a saturated calomel electrode in pH 7.0 buffer solution, corresponding to $\text{heme}Fe^{III}+e\rightarrow\text{heme}Fe^{II}$. Some electrochemical parameters were calculated by performing nonlinear regression analysis of square wave voltammetry (SWV) experimental data. The formal potential was linearly dependent on pH, indicating the electron transfer of Fe^{III}/Fe^{II} redox couple accompanied by the transfer of proton. Ultraviolet visible and Fourier transform infrared spectra suggested that the conformation of proteins in the PNM films retained the essential feature of its native secondary structure. Atomic force microscopy images demonstrated the existence of interaction between heme proteins and PNM. *N*,*N*-dimethylformamide (DMF) played an important role in immobilizing proteins and enhancing electron transfer between proteins and electrodes. Electrochemical catalytic reductions of hydrogen peroxide and trichloroacetic acid by proteins entrapped in PNM film were also discussed, showing the potential applicability of the film modified electrodes as a biosensor.

Keywords: Heme proteins; PNM; Direct electrochemistry; Electrocatalysis; Biosensor

1. Introduction

Direct electron transfer between proteins and electrodes not only can provide a good model for mechanistic studies of electron transfer in real biological systems, but also establishes a foundation for fabricating biosensors, biomedical devices, and enzymatic bioreactors [1,2]. So the direct electrochemistry of proteins has an important significance as it was used to design and construct the third generation biosensors without mediators or promoters.

A relatively new approach to realize direct electrochemistry of proteins was to entrap proteins into films that were modified on electrode surface [3–5]. In recent years, silica sol–gel material has emerged as one matrix well suitable for the immobilization of proteins [6,7]. This kind of inorganic silica sol–gel material can be prepared under ambient conditions and exhibits tunable porosity, high thermal stability, chemical inertness and negligible swelling in both aqueous and non-aqueous solutions [8,9]. However, silica sol–gel derived matrix was fragile and can easily shrink, crack and desquamate from the electrode surface [9]. Meanwhile, the silica sol–gel process was usually carried out in acidic condition, which was hostile to the activities of proteins. The organic polymer components were rigorously introduced into the starting solution under low humidity conditions, and the substrates coated with sol–gel usually need to be calcined at high temperature [10] which is also not beneficial to the activities of proteins. New sol–gel materials are essential for biosensor construction. Huang [11] reported the synthesis and characterization of linear poly (*N*-isopropylacyamide-co-3-methacryloxypropyltrimethoxy silane) (PNM), which was water-soluble and becomes a hydrogel under extra-wild conditions. Compared to the characteristic of the

* Corresponding author. Ministry-of-Education Key Laboratory for the Synthesis and Application of Organic Functional Molecules, PR China. Tel.: +86 27 50865498; fax: +86 27 88663043.
E-mail address: wangsf@hubu.edu.cn (S.-F. Wang).

1567-5394/$ - see front matter © 2007 Elsevier B.V. All rights reserved.
doi:10.1016/j.bioelechem.2007.04.004

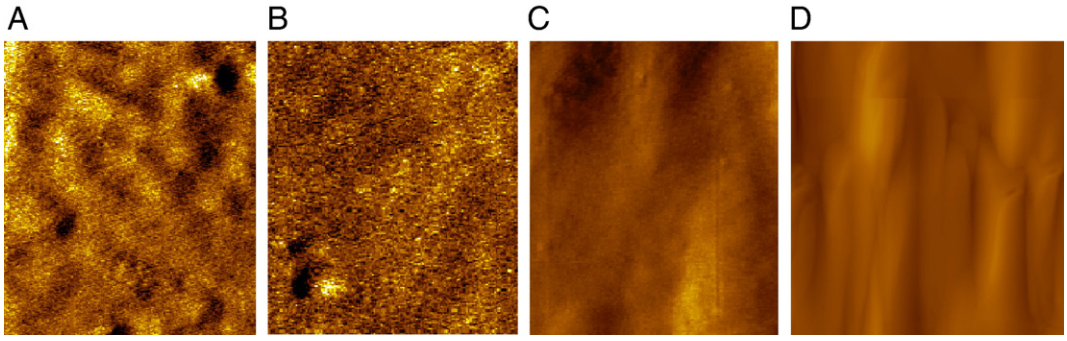

Fig. 1. AFM images of (A) PNM; (B) PNM+DMF (C) PNM–Hb; (D) PNM–Hb+DMF on HOPG surface; 2000 nm×2000 nm.

above-mentioned sol–gel material, the polymer has several advantages such as water solubility, biocompatibility, and good film forming ability at room temperature in nearly moderate pH conditions. We thus expect that the PNM provides a new and different matrix for immobilization of proteins or enzymes, and creates a suitable microenvironment for redox proteins to exchange electron directly with underlying electrodes.

In this paper, myoglobin (Mb), hemoglobin (Hb) and Catalase (Cat) were incorporated in PNM film modified on glass carbon (GC) electrodes. Direct electrochemistry of protein–PNM films was studied in detail. The protein–PNM films were also characterized by UV–vis spectroscopy (UV–vis), FTIR Spectra (FTIR), atomic force microscopy (AFM) and AC impedance. Electrochemical catalytic reductions of hydrogen peroxide (H_2O_2) and trichloroacetic acid (TCA) were also discussed, showing the potential applicability of the film modified electrodes as a biosensor.

2. Experiment

2.1. Chemicals

Cattle hemoglobin and horse heart myoglobin were from Fluka. Catalase was from Sigma. PNM was from Prof. Huang of Wuhan University, China. Hydrogen peroxide (H_2O_2, 30%) was from Beijing Chemical Engineering Plant. A stock solution of H_2O_2 (0.050 mol L^{-1}) was prepared. The solution was standardized by titration with potassium permanganate. Testing standard solutions were prepared daily by appropriate dilution of the stock solution. All other chemicals were reagent grade. All of the chemicals were used as received. All the water used in the experiments was deionized and was purified twice successively by ion exchange and distillation.

Buffer solutions for voltammetry all contained 100 mM KBr. Buffer solutions were 25 mM citrate for pH 3.0–6.0, 25 mM phosphate for pH 7.0–8.0, and 25 mM borate for pH 9.0–10.0.

2.2. Apparatus and methods

Electrochemical measurements were performed at a CHI660 electrochemistry workstation (CH Instruments Co., USA). The electrochemical cell consisted of a three-electrode system where the modified glass carbon electrode (d=3 mm) was used as the working electrode, a platinum wire as the counter electrode and a saturated calomel electrode (SCE) as the reference electrode. All measurements were carried out at room temperature.

All experimental solutions were deaerated by bubbling highly pure nitrogen for 15 min, and a nitrogen atmosphere was kept over the solution during measurements.

UV–vis spectra were recorded with a Perkin-Elmer Lambda 17 UV–visible spectrophotometer with a wavelength range of 190–900 nm (Perkin Elmer, USA). FTIR spectrometer instrument was purchased from Perkin Elmer Co. (USA). All the spectra were obtained with an average of 100 scans with 4 cm^{-1} resolution. AFM images were obtained on a PicoScan system (Molecular Imaging Inc., USA) operated in contact mode with commercially ultra-sharpened Si_3N_4 tips (MAClever II, Molecular Imaging Inc., USA). In each measurement, the set point was adjusted to minimize the force between the tip and the sample immobilized on high-ordered pyrolytic graphite (HOPG, ZYH, Advanced Ceramics Co., USA).

2.3. Electrode modification

Prior to coating, GC electrodes were polished with 0.05 μm alumina and sonicated three times in deionized water. They were then treated in 1:1 (v/v) aqueous nitric acid for 10 min, followed by rinsing and sonication in water and methanol successively.

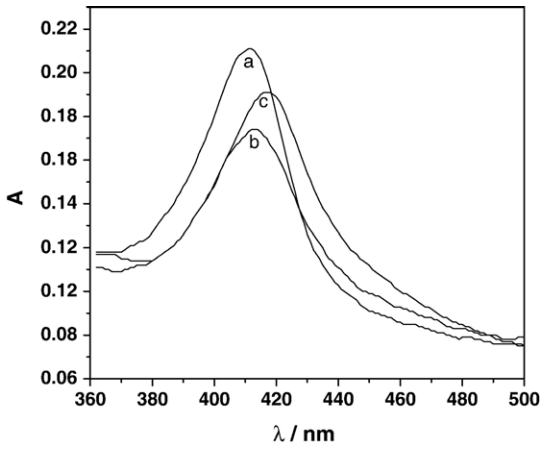

Fig. 2. UV–vis absorption spectra of Mb and Mb–PNM films on glass slides for: (a) dry Mb film; (b) dry Mb–PNM film; (c) dry Mb–PNM+DMF film.

Table 1
Wavelengths of the Soret absorption bands for heme protein–PNM films (nm)

Proteins	Protein films	Protein–PNM films	Protein–PNM+DMF films
Hb	412	414	418
Mb	413	414	417
Cat	408	414	416

A PNM solution (0.1 g mL^{-1}) was prepared by dissolving the PNM in an aqueous solution in the refrigerator (4 °C) for 30 min. The concentration of the proteins stock solutions, prepared by dissolving proteins in 0.05 M phosphate buffer solution (pH 7.0), was 10, 10, and 30 g L^{-1} for Hb, Mb, and Cat, respectively. A 15 μL volume of PNM and 10 μL of DMF were mixed with 15 μL of the protein stock solution, and then 20 μL of the mixture was pipetted onto the surface of the pretreated GC and spread gently over the entire surface. A small bottle was fit tightly over the electrode so that water evaporated slowly and more uniform films were formed. The films were then dried in air overnight. The PNM film modified electrode was prepared in the same way as described above but without proteins.

3. Results and discussions

3.1. Characterization of proteins immobilization

3.1.1. AFM

The morphologies of PNM and protein–PNM films measured by AFM were compared. Fig. 1 presents the AFM images of PNM film (Fig. 1A), PNM+DMF film (Fig. 1B), Hb–PNM film (Fig. 1C) and Hb–PNM+DMF film (Fig. 1D). The image of PNM film (Fig. 1A) and Hb–PNM film (Fig. 1C) containing no DMF on the HOPG surface looked loose and uneven, with some protrusions assignable to Hb molecules in the PNM films. However, the distribution of Hb in the PNM film was not uniform (Fig. 1C). After the addition of DMF, The PNM+DMF film (Fig. 1B) surface became compact and uniform compared to PNM-film (Fig. 1A), suggesting that a gelatification process of PNM was enhanced by DMF. Fig. 1D is the morphology of Hb–PNM+DMF film; a uniform, stable and chain-like Hb–PNM film can be observed, and the results were the same as those of Boussaad and Tao [12]. The films may weaken the congregation of protein on bare GC electrodes and expose the heme crevice to a more hydrophobic environment with the addition of DMF, thus lowering the reorganization energy for electron transfer [13].

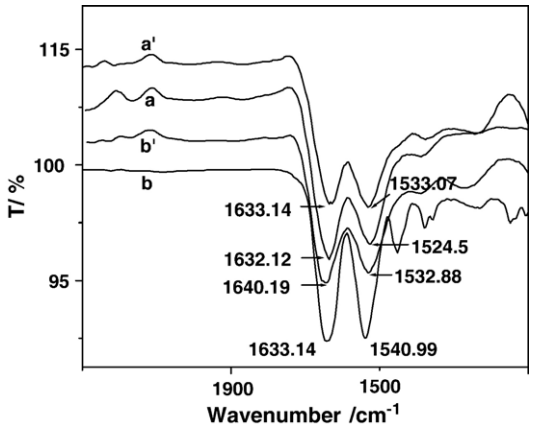

Fig. 4. FTIR spectra for (a) Cat film, (a′) Cat–PNM film, (b) Hb film, (b′) Hb–PNM film.

3.1.2. UV–vis spectroscopy

The locations of the Soret absorption band of iron heme may provide information about the denaturation of heme proteins. When heme proteins were denatured, the Soret band shifted or disappeared [14]. UV–vis spectroscopy was thus used here to detect the change of Soret band of proteins in PNM films cast on the glass slides. In this study, the proteins concentration and the ratio of proteins to PNM and DMF were the same for both UV–vis spectroscopy and electrochemical experiments. Taking Mb–PNM film as an example, dry films cast from Mb and Mb–PNM and Mb–PNM+DMF solutions showed Soret bands at 413, 414, and 417 nm (Fig. 2a, b and c), respectively. This suggests that Mb in dry-PNM films has a secondary structure nearly the same as the native state of Mb in its dry films alone and no significant denaturation has occurred for Mb–PNM films containing DMF. The Soret absorption bands of the heme proteins are summarized in Table 1.

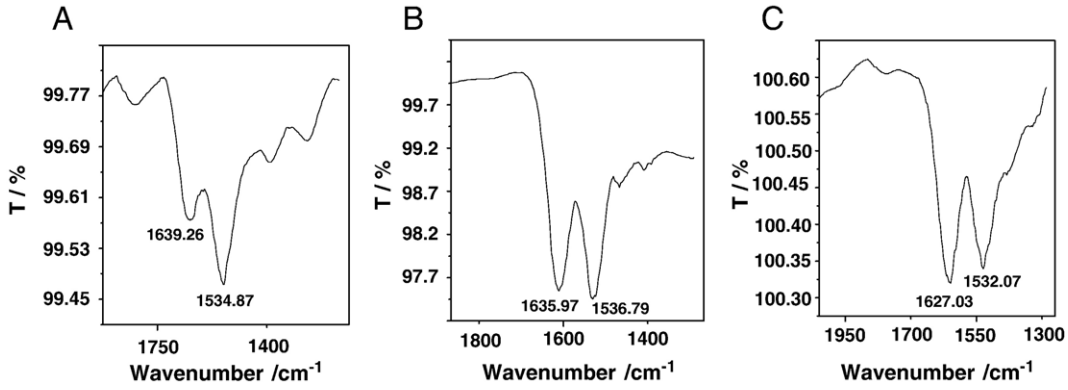

Fig. 3. FTIR spectra for (A) Mb film, (B) Mb–PNM film, (C) Mb–PNM+DMF film.

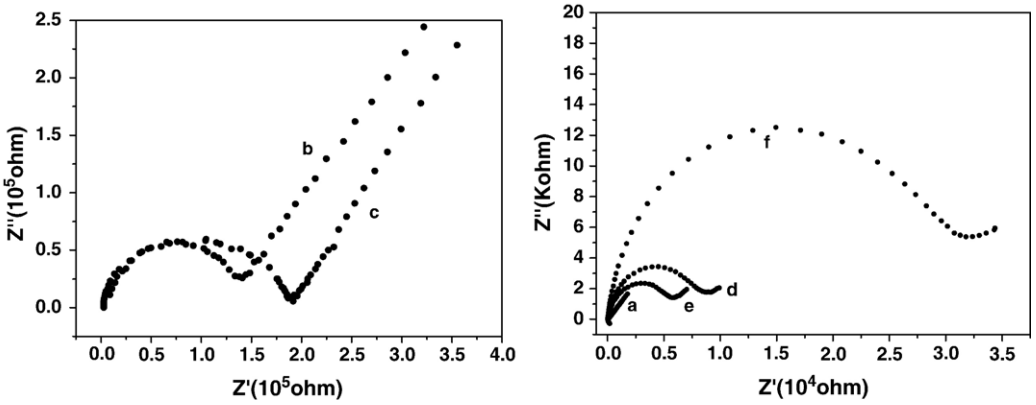

Fig. 5. AC impedance plots of GC (a); PNM (b); PNM+DMF (c); Hb–PNM (d); Hb–PNM+DMF (e) and Hb (f) in the presence of 0.5 mmol L^{-1} $[Fe(CN)_6]^{3-}$ + 0.5 mmol L^{-1} $[Fe(CN)_6]^{4-}$ + 0.5 mol L^{-1} KNO_3 as the supporting electrolyte. The electrode potential was 0.22 V; the frequency range was 0.1 Hz to 10^5 super Hz.

3.1.3. FTIR spectroscopy

FTIR spectral band shapes can be used to monitor changes in protein conformation [15,16]. The shapes of amide I (1700–1600 cm^{-1}) and amide II (1600–1500 cm^{-1}) infrared absorption bands of proteins provide detailed information on the secondary structure of the polypeptide chain [17]. Fig. 3 shows the amide I and amide II bands of Mb in Mb–PNM film (1635.97 cm^{-1} and 1536.79 cm^{-1}) (Fig. 3B) are very similar to those obtained in the protein spectrum (1639.26 cm^{-1} and 1534.87 cm^{-1}) (Fig. 3A); the similarity of spectra in Fig. 3A and B suggests that Mb retains the essential features of its original structure in the PNM film. When DMF was added to the Mb–PNM film, the amide I and amide II bands of Mb in the FTIR spectra shifted to 1627.03 cm^{-1} and 1532.07 cm^{-1} (Fig. 3C), respectively. This suggests that the addition of DMF strengthened the hydrophobicity of the microenvironment. The amide I and amide II bonds of the other two proteins themselves and proteins in PNM films are shown in Fig. 4. The similarities of the two spectra above indicate that protein retains the essential feature of its native secondary structure in the PNM-films.

3.1.4. Impedance

Fig. 5 shows some alternative current impedance recorded in given conditions. Impedance can give information on the impedance changes of the electrode surface in the modification process. When the GC electrode was coated by PNM, the locus curves diameter (Fig. 5b) increased obviously. PNM/GC electrode showed a higher interfacial electron transfer resistance ($R_{ct}=1.75\times10^5\,\Omega$) compared with the bare GC electrode (Fig. 5a), indicating that the PNM-film resisted electron transfer of the electrochemical probe. PNM+DMF film, the R_{ct} value of the PNM+DMF/GC (Fig. 5c) further increased to $2.00\times10^5\,\Omega$, suggesting that the film became more compact and uniform due to the addition of DMF; this is in agreement with the results of AFM above. We observed that the R_{ct} (Fig. 5f) increased largely upon spreading of Hb to GC electrode surface compared to bare GC electrode. The PNM-film could decrease the R_{ct} of Hb (Fig. 5d) because it avoided the Hb molecules adsorbed on the bare GC electrode surface for subsequent denaturation and passivation. While DMF may strengthen the hydrophobicity of the micro-environment of protein and form a cavity and favor electron transfer of electrochemical probe and further decrease the R_{ct} (Fig. 5e) of Hb–PNM+DMF/GC, this is beneficial for the electron transfer of proteins, and hence the redox reaction of Hb could easily take place on Hb–PNM+DMF/GC.

3.2. Direct electrochemical properties of protein–PNM film electrodes

3.2.1. Cyclic voltammetry

Protein–PNM film electrodes were immersed into pH 7.0 buffer solution; after several CV scans, a pair of well-defined, quasi-reversible CV peaks at about −0.35 V was observed for

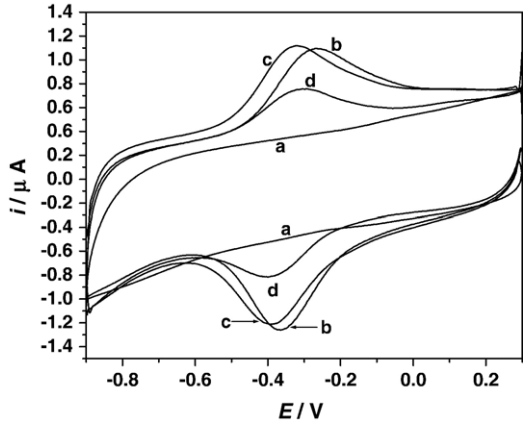

Fig. 6. Cyclic voltammograms at 0.2 V s^{-1} in pH 7.0 buffer solution for: (a) PNM/GC; (b) Hb–PNM/GC; (c) Mb–PNM/GC; (d) Cat–PNM/GC films.

Table 2
Electrochemical parameters of protein–PNM films

Films	$E^{0\prime}$ (V)	CV $\Gamma\times10^{11}$ (mol cm^{-2})	$E^{0\prime}$ (V)	SWV $\Gamma\times10^{11}$ (mol cm^{-2})	k_s (s^{-1})	α
Hb–PNM	−0.35	2.07	−0.343	1.56	16	0.496
Mb–PNM	−0.36	1.94	−0.344	2.60	20	0.50
Cat–PNM	−0.36	1.43	−0.311	0.98	17.0	0.51

SWV conditions for Hb: pulse height 60 mV and frequencies (Hz): (a) 122, (b) 143, (c) 161, (d) 185.
Mb and Cat: pulse height 75 mV and frequencies (Hz): (a) 132, (b) 152, (c) 172, (d) 185.

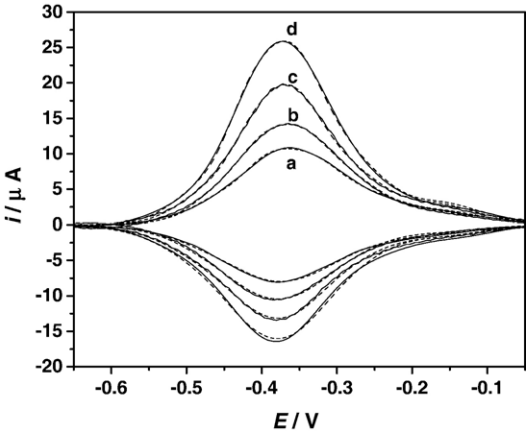

Fig. 7. Square wave forward and reverse current voltammograms for Cat–PNM films in pH 7.0 buffer solution at different frequencies. The solid lines represent the experimental SWV from which background has been subtracted. Points are the best fit by nonlinear regression onto the 5-$E^{0\prime}$ dispersion model. SWV conditions: pulse height 60 mV and frequencies (Hz): (a) 132, (b) 152, (c) 172, (d) 185.

both protein–PNM films (Fig. 6b–e). The peaks were located at the potentials characteristic of the heme Fe^{III}/Fe^{II} redox couples of the proteins [18]. No redox peaks were observed at PNM modified GC electrode in the same potential range (Fig. 6a). The redox peak pairs of the heme protein–PNM films had an approximately symmetric peak shape and nearly equal heights of reduction and oxidation peaks. The reduction and oxidation peak currents for immobilized heme proteins were found to increase linearly with scan rates from 0.05 to 1 V s^{-1}. Integration of reduction peaks gave nearly constant charge (Q) values with different scan rates. The logarithm plot of cathodic peak current of Mb versus logarithm of scan rate gives a linear relationship with a correlation coefficient of 0.9991 and a slope of 0.934, which is very close to the theoretical slope of 1 for thin layer voltammetry [19]. All these are characteristic of quasi-reversible, surface electrochemistry in which all electroactive proteins in the films have been reduced on the forward cathodic scan, with full conversion of the reduced proteins back to their oxidized forms on the reversed anodic scan [20,21]. According

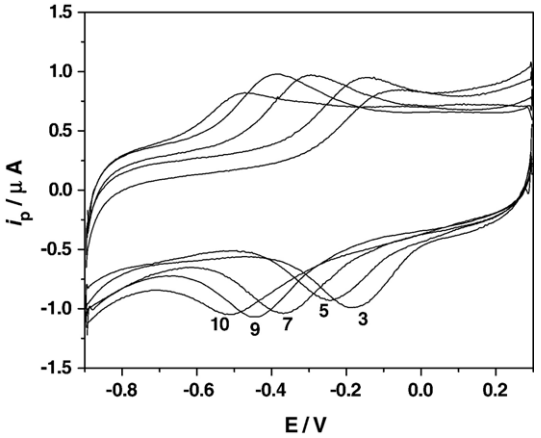

Fig. 8. Cyclic voltammograms of Mb–PNM/GC in 0.1 M buffer solution at different pHs. Scan rate: 0.2 V s^{-1}.

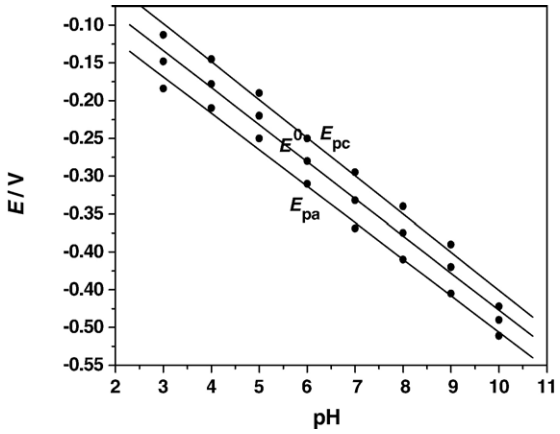

Fig. 9. Plots of E vs. pH.

to the Q–Γ relationship [20], the surface concentrations of electroactive proteins in the films (Γ) are shown in Table 2.This value was below the total amount of proteins deposited on the electrode surface and suggests that only those proteins in the inner layer of the films close to the electrode and with a suitable orientation can exchange electrons with the electrode.

3.2.2. Square wave voltammetry and estimation of electrochemical parameters

The average formal potentials ($E^{0\prime}$) and apparent heterogeneous electron transfer rate constants (k_s) were estimated by employing nonlinear regression analysis of SWV forward and reverse curves [22,23]. An example is shown in Fig. 7. The results calculated are also listed in Table 2. $E^{0\prime}$ values estimated as a midpoint of CV reduction and oxidation peak potential for the films are also listed, which are in good agreement with those obtained by SWV.

The stability of protein–PNM/GC film electrodes was tested by CV. Protein–PNM/GC film electrodes were stored in pH 7.0 blank buffer solution in the refrigerator at 4 °C, and CV tests were carried out periodically and showed excellent stability. For Hb and Mb, the peak potentials and currents remained unchanged for 1 month; it retained 80% of initial current response after 3 months. Compared to these two protein–PNM films, Cat–PNM film seemed to be less stable. The peak current of Cat–PNM films decreased to about 10% of its initial steady state after 1 month of storage in buffer solution in the refrigerator at 4 °C. Good long-term stability was mainly attributed to the mild immobilization process of proteins. The processes of

Table 3
Effect of pH (3.0–10.0) on E_{pa}, E_{pc} and $E^{0\prime}$

Film	pH	Regression equations (correlation coefficients: 0.997–0.999)		
Hb–PNM	3.0–10.0	E_{pa}=−0.029–0.0422 pH	E_{pc}=−0.128–0.0382 pH	$E^{0\prime}$=0.0784–0.0402 pH
Mb–PNM	3.0–10.0	E_{pa}=0.053–0.050 pH	E_{pc}=−0.024–0.048 pH	$E^{0\prime}$=0.0135–0.0491 pH
Cat–PNM	5.0–10.0	E_{pa}=−0.062–0.052 pH	E_{pc}=−0.100–0.041 pH	$E^{0\prime}$=−0.0183–0.047 pH
Cat–PNM	3.0–5.0	E_{pa}=−0.096–0.021 pH	E_{pc}=−0.164–0.029 pH	$E^{0\prime}$=−0.132–0.024 pH

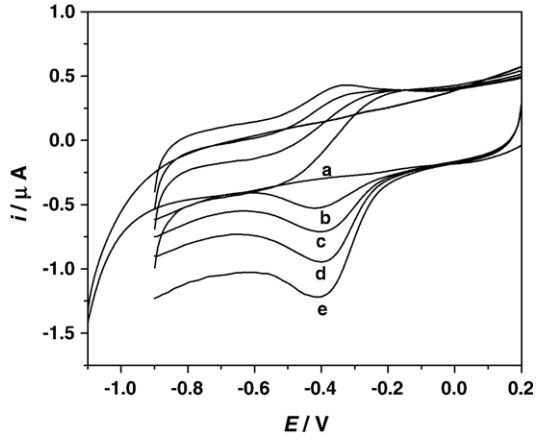

Fig. 10. Cyclic voltammograms at 0.1 V s^{-1} in pH 7.0 buffers for Mb–PNM film in buffer solution containing no (b) H_2O_2, (c) 3.39 μM, (d) 5.08 μM, and (e) 8.47 μM H_2O_2. (a) PNM film in buffer solution containing 5.08 mM H_2O_2.

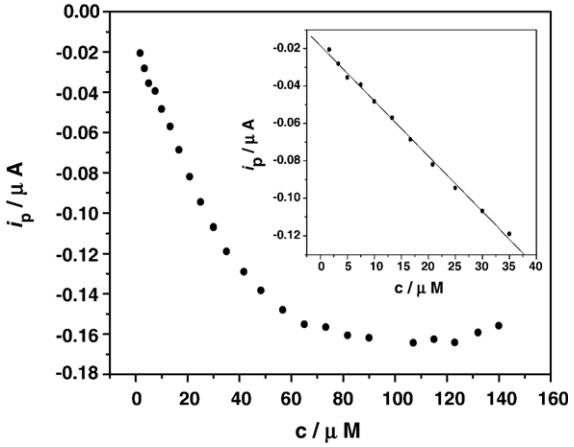

Fig. 12. The calibration plots of the catalytic peak current of Cat–PNM film to H_2O_2 concentration. Inset shows the linear range of the biosensor response.

electrode modification avoid the shortcomings caused by acidic catalyst or calcinations step needed in traditional sol–gel process [24,25] and maintain their biological activity to a large extent.

3.2.3. Influence of pH on electrochemical behaviors

An increase of pH of the solution leads to a negative shift in potential for both cathodic and anodic CV peaks for protein–PNM films. Nearly reversible voltammograms with stable and well-defined redox peaks were obtained for four proteins in the pH range of 3.0–10.0. Fig. 8 shows the CVs of Mb immobilized in PNM films in pH 3.0–10.0. When the pH values were adjusted to below 4.0, the CV graphs became asymmetric and the cathodic current increased remarkably compared to that obtained at pH values above 4.0. This was likely due to the conformational change of protein in acidic solution. The UV–vis also confirmed this point.

The formal potentials ($E^{0\prime}$) had a linear relationship with pH (3.0–10.0) (Fig. 9). The linear regression equations are listed in Table 3. All these slope values are smaller than the theoretical value of 57.6 mV pH^{-1} at 18 °C for a single-proton coupled, reversible one-electron transfer [26,27]. The reason might be the influence of the protonation states of trans ligands to the heme iron and amino acids around the heme, or the protonation of the water molecule coordinated to the central iron [28].

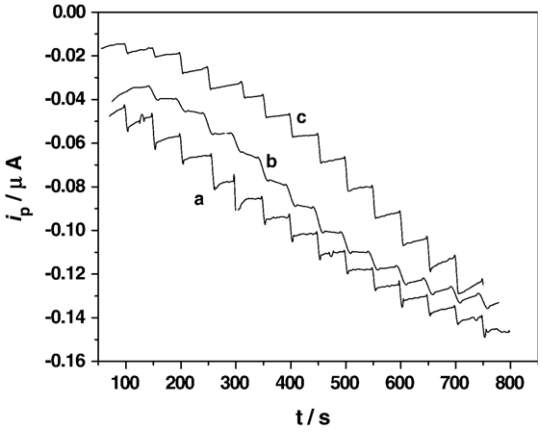

Fig. 11. Typical current–time response curve of the sensor upon successive additions of (a) 5, 5, 10, 10, 15, 15, 20, 20, 25, 25, 30, 30, 35, 35 μL 2.5 × 10^{-3} mol L^{-1} H_2O_2; (b) 10 μL every time 2.5 × 10^{-3} mol L^{-1} H_2O_2; (c) 5, 5, 10, 10, 15, 15, 20, 20, 25, 25, 30, 30, 40 μL 2.5 × 10^{-3} mol L^{-1} H_2O_2 to 15.00 mL pH 7.0 buffer solution at −0.25 V.

3.3. Electrocatalytic activity

Electrocatalytic behaviors of protein–PNM films were tested with various substrates such as hydrogen peroxide (H_2O_2) and trichloroacetic acid (TCA).

For electrocatalytic reduction of H_2O_2, we took Mb–PNM film electrodes as an example. When H_2O_2 was added to a pH 7.0 buffer solution, compared with the system with no H_2O_2 present, an obvious increase in the reduction peak at about −0.4 V was observed with the disappearance of the oxidation peak (Fig. 10c, d). However, direct reduction of H_2O_2 at blank film electrodes was not observed (Fig. 10a), indicating that Mb entrapped in PNM film catalyzed the reduction of H_2O_2.

In order to evaluate the dependence of the electrocatalytic current of the protein–PNM/GC electrode on the concentration of H_2O_2, chronoamperometric experiments (at a constant potential of −0.25 V) were carried out. Fig. 11 shows the electrocatalytic current of the protein–PNM/GC electrode increase with each addition of H_2O_2 to the solution. The current reaches its maximum value within 4, 5, and 8 s for Hb (a), Mb (b) and Cat (c), respectively, suggesting that the protein–PNM/GC electrode can

Table 4
Relationships between catalytic currents and H_2O_2 concentrations

Films	Concentration range	Linear regression equations	Correlation coefficients	Response time(s)
Hb–PNM	0.19–1.53 μM	I/μA = −0.050–0.051 c/μM	0.9981	4
Mb–PNM	0.19–1.53 μM	I/μA = −0.046–0.054 c/μM	0.9954	8
Cat–PNM	1.67–35.2 μM	I/μA = −0.018–0.0029 c/μM	0.9984	5

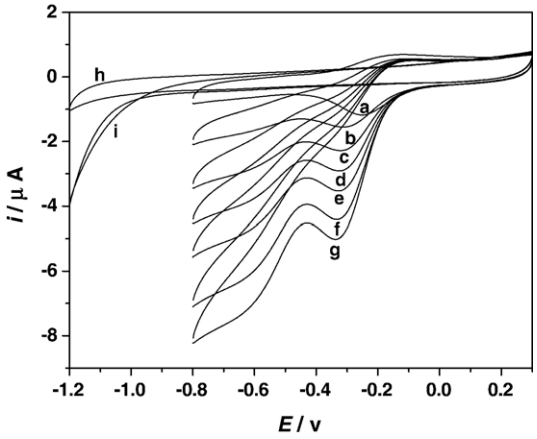

Fig. 13. Cyclic voltammograms at 0.1 V s^{-1} in pH 3.0 buffer solution for Hb–PNM film in buffer solution containing (a) 0; (b) 7.43 mM; (c) 11.14 mM; (d) 14.86 mM; (e) 18.58 mM; (f) 22.29 mM; (g) 26 mM TCA. (h) PNM film in buffer solution containing no TCA and (i) PNM film in buffer solution containing 14.86 mM TCA.

respond rapidly to changes in the concentration of H_2O_2. The reduction peak current increases with the concentration of H_2O_2 in solution (Fig. 12). The calibration curve tends to level off and even slope down with the addition of H_2O_2, indicating a progressive inactivation of Hb in the presence of higher concentrations of H_2O_2. Fig. 12 inset shows the amperometric current of Cat–PNM film had a good linear relationship with the concentration of H_2O_2. The same results were also obtained for Hb–PNM film and Mb–PNM film (Table 4).

The electrocatalytic reduction of TCA by protein–PNM films was also tested by CV. Using Hb–PNM film as an example, after TCA was added to a pH 3.0 buffer solution, the Hb–Fe^{III} reduction peak of Hb–PNM films at about −0.3 V increased in height (Fig. 13b), accompanied by a decrease in the $HbFe^{II}$ oxidation peak. Compared to direct reduction of TCA on PNM films without Hb at the potential more negative than −1.0 V (Fig. 13i), Hb–PNM films lowered the reduction overpotential of TCA by at least 0.7 V. These results are characteristic of electrochemical catalysis, where $HbFe^{II}$, the reduction product of the electrode reaction, was oxidized by TCA in a chemical reaction and returned to Hb–Fe^{III} form, forming a catalytic cycle. TCA maybe underwent a stepwise reduction dechlorination to ultimately become acetic acid. These results are consistent with those of Rusling and Hu [29,30]. The catalytic reduction peak current had a linear relationship with TCA concentration in the range of 1.486×10^{-3}–1.114×10^{-2} mol L^{-1}, with a correlation coefficient of 0.998; the other protein–PNM films showed very similar catalytic property toward TCA.

4. Conclusions

Stable heme protein–PNM film modified electrodes were fabricated. Heme proteins entrapped in PNM film could transfer electrons directly with underlying electrodes, corresponding to the redox couple of Fe^{III}/ Fe^{II}. UV–vis and FTIR spectra suggest that the proteins can retain their original conformation in PNM film. DMF plays an important role in immobilizing the proteins and enhancing the electron transfer between the proteins and the electrodes. Good electrocatalytic properties of the protein–PNM films toward various substrates are of biological or environment significance. The good stability of protein–PNM films indicates that it has a promising potential in the fabrication of new generation biosensors or bioreactors based on the direct electrochemistry of proteins.

Acknowledgements

The authors wish to thank Prof. J.F. Rusling and Prof. D.W. Pang for providing the software for nonlinear regression analysis of SWV data. This work was supported by the National Nature Science Foundation of China (No. 20575017).

References

[1] M.F. Chaplin, C. Bucke, Enzyme Technology, Cambridge University Press, Cambridge, UK, 1990.
[2] F.A. Armstrong, H.A.O. Hill, N.J. Walton, Direct electrochemistry of redox proteins, Acc. Chem. Res. 21 (1988) 407–413.
[3] Y. Xie, H.Y. Liu, N.F. Hu, Layer-by-layer films of hemoglobin or myoglobin assembled with zeolite particles: electrochemistry and electrocatalysis, Bioelectrochemistry 71 (2006) 6–14.
[4] Q. Lu, S.S. Hu, Studies on direct electron transfer and biocatalytic properties of hemoglobin in polytetrafluo-roethylene film, Chem. Phys. Lett. 424 (2006) 167–171.
[5] X. Ma, X.J. Liu, H. Xiao, G.X. Li, Direct electrochemistry and electrocatalysis of hemoglobin in poly-3-hydroxybutyrate membrane, Biosens. Bioelectron. 20 (2005) 1836–1842.
[6] Z.H. Dai, X.X. Xu, H.X. Ju, Direct electrochemistry and electrocatalysis of myoglobin immobilized on a hexagonal mesoporous silica matrix, Anal. Biochem. 332 (2004) 23–31.
[7] T. Yao, K. Takashima, Amperometric biosensor with a composite membrane of sol–gel derived enzyme film and electrochemically generated poly (1,2-diaminobenzene) film, Biosens. Bioelectron. 13 (1998) 67–73.
[8] J. Wang, Sol–gel materials for electrochemical biosensors, Anal. Chim. Acta 399 (1999) 21–27.
[9] O. Lev, M. Tsionsky, L. Rabinovich, V. Glezer, S. Sampath, I. Pankratov, J. Gun, Anal. Chem. 67 (1995) 22A.
[10] T. Yoko, L. Hu, H. Kozuka, S. Sakka, Photoelectrochemical properties of TiO_2 coating films prepared using different solvents by the sol–gel method, Thin Solid Films 283 (1996) 188–195.
[11] J.T. Zhang, S.W. Huang, R.X. Zhuo, A novel sol–gel strategy to prepare temperature-sensitive hydrogel for encapsulation of protein, Colloid Polym. Sci. 284 (2005) 209–213.
[12] S. Boussaad, N.J. Tao, Electron transfer and adsorption of myoglobin on self-assembled surfactant films: an electrochemical tapping-mode AFM study, J. Am. Chem. Soc. 121 (1999) 4510–4515.
[13] B.R. Van Dyke, P. Saltman, F.A. Armstrong, Control of myoglobin electron-transfer rates by the distal (nonbound) histidine residue, J. Am. Chem. Soc. 118 (1996) 3490–3492.
[14] P. George, G.I.H. Hanania, Spectrophotometric study of ionizations in methemoglobin, J. Biochem. 55 (1953) 236–243.
[15] H. Susi, D.M. Byler, Resolution-enhanced Fourier transform infrared spectroscopy of enzymes, Methods Enzymol. 130 (1986) 290–311.
[16] K. Niwa, M. Furukawa, K. Niki, Ir reflectance studies of electron transfer promoters for cytochrome c on a gold electrode, J. Electroanal. Chem. 245 (1988) 275–285.
[17] T.G. Spiro, T.C. Strekas, Resonance Raman spectra of heme proteins. Effects of oxidation and spin state, J. Am. Chem. Soc. 96 (1974) 338–345.
[18] Z. Zhang, S. Chouchane, R.S. Magliozzo, J.F. Rusling, Direct voltammetry and catalysis with Mycobacterium tuberculosis catalase–peroxidase, peroxidases, and catalase in lipid films, Anal. Chem. 74 (2002) 163–170.

[19] A.J. Bard, L.R. Faulkner, Electrochemical Methods, Wiley, New York, 1980, pp. 54–55.
[20] R.W. Murray, in: A.J. Bard (Ed.), Electroanalytical Chemistry, vol. 13, Marcel Dekker, New York, 1984, pp. 191–368.
[21] L. Shen, R. Huang, N. Hu, Myoglobin in polyacrylamide hydrogel films: direct electro-chemistry and electrochemical catalysis, Talanta 56 (2002) 1131–1139.
[22] J.J. O'Dea, J.G. Osteryoung, Characterization of quasi-reversible surface processes by square-wave voltammetry, Anal. Chem. 65 (1993) 3090–3097.
[23] A.E.F. Nassar, Z. Zhang, N. Hu, J.F. Rusling, T.F. Kumosinski, Proton-coupled electron transfer from electrodes to myoglobin in ordered biomembrane-like films, Phys. Chem. Earth, Part B Hydrol. Oceans Atmos 101 (1997) 2224–2231.
[24] Z.T. Jiang, Y.M. Zuo, Synthesis of porous titania microspheres for HPLC packings by Polymerization-Induced Colloid Aggregation (PICA), Anal. Chem. 73 (2001) 686–688.
[25] E. Milella, F. Cosentino, A. Licciulli, C. Massaro, Preparation and characterisation of titania/hydroxyapatite composite coatings obtained by sol–gel process, Biomaterials 22 (2001) 1425–1431.
[26] A.M. Bond, Modern Polarographic Methods In Analytical Chemistry, Marcel Dekker, New York, 1980, pp. 29–30.
[27] L. Meites, Polarographic Techniques, second ed., Wiley, New York, 1965, pp. 282–284.
[28] I. Yamazaki, T. Araiso, Y. Hayashi, H. Yamada, R. Makino, Analysis of acid–base properties of peroxidase and myoglobin, Adv. Biophys. 11 (1978) 249–281.
[29] A.E.F. Nassar, J.M. Bobbitt, J.O. Stuart, J.F. Rusling, Catalytic reduction of organohalide pollutants by myoglobin in a biomembrane-like surfactant film, J. Am. Chem. Soc. 117 (1995) 10986–10993.
[30] H. Sun, N.F. Hu, Voltammetric studies of hemoglobin-coated polystyrene latex bead films on pyrolytic graphite electrodes, Biophys. Chem. 110 (2004) 297–308.